PHYSICAL REVIEW B VOLUME 28, NUMBER 12 15 DECEMBER 1983

Electronic structure of Cr silicides and Si-Cr interface reactions

A. Franciosi and J. H. Weaver
Department of Chemical Engineering and Materials Science, University of Minnesota, Minneapolis, Minnesota 55455

D. G. O'Neill
Synchrotron Radiation Center, University of Wisconsin, Stoughton, Wisconsin 53589

F. A. Schmidt
Ames Laboratory—U.S. Department of Energy, Iowa State University, Ames, Iowa 50011

O. Bisi and C. Calandra
Istituto di Fisica, Università degli Studi di Modena, I-4110 Modena, Italy
(Received 12 August 1983)

We present synchrotron radiation photoemission studies of bulk $CrSi_2$ and silicide phases grown on Si by thermal processing of the Si-Cr interface. Experiment shows that Si-Cr interface formation at room temperature results in reacted phases that differ from both bulk $CrSi_2$ and *in situ*—grown Si-rich $CrSi_2$. Extended—Hückel-theory linear combination of atomic orbitals calculations of the density of states of Cr_3Si, CrSi, and $CrSi_2$ show that Si—Cr bond formation involves Si p and Cr d states with minimal charge transfer.

I. INTRODUCTION

The formation of refractory metal silicides by heat treatment of silicon-metal interfaces offers promise of widespread application in integrated circuit technology,[1] but the mechanisms that drive interface formation and silicide nucleation are not well understood.[2,3] In part, this is because of limited microscopic information about the electronic and structural properties of interfaces as they evolve during thermal processing.[4–7] Further, there is inadequate understanding of silicides themselves[8–12] and the parameters which influence their bulk properties, including stoichiometry, disorder, segregation, and chemical bonding. In this paper, we focus on the Cr-Si interface and try to resolve some of these uncertainties by examining bulk $CrSi_2$, by following the evolution of interface reaction products as a function of temperature, and by comparing with density of states calculations.

In an earlier investigation of the Si(111)2×1-Cr interface we showed that room-temperature reaction produces intermixed Si-Cr phases for metal coverages of less than 10 monolayers.[11,12] Electronic structure calculations for Cr silicides in simplified lattice structure allowed us to identify trends related to bond formation and stoichiometry variations.[12] The present study extends that work. Important new insight in the silicide electronic structure is obtained through semiempirical calculations for Cr_3Si, CrSi, and $CrSi_2$ in their actual crystal structure, including the amount of Si-Cr p-d hybridization, the energy position and width of the nonbonding $3d$ features, and the role of ionicity in the bond. Experimental results for bulk $CrSi_2$ are then understood in terms of substantial p-d hybridization and the reduction of the $3d$-$3d$ interaction relative to pure Cr. Comparison with the interface data indicates both similarities and important differences. Temperature-dependent studies show the evolution of $CrSi_2$ and, ultimately, Si segregation at the surface.

II. EXPERIMENTAL

The bulk $CrSi_2$ samples were prepared from ultrapure Iochrome Cr (99.99% purity with less than 100 ppm total impurities) and Dow Corning Si (resistivity of 1000 Ω cm). The starting materials were first arc melted then directionally melted by rf heating using a horizontal cold crucible technique to promote homogeneity and grain growth. Analysis of the resulting $CrSi_2$ ingot showed 48.02 wt. % chromium with lattice constants of $a=4.4277\pm0.0001$ Å and $c=6.3691\pm0.0004$ Å (hexagonal $C40$ lattice) compared to the target value of 48.07 wt. % and lattice constants of 4.436 and 6.369 Å for Cr-rich $CrSi_2$ and 4.428 and 6.363 Å for Si-rich $CrSi_2$. (For further crystallographic information see Table I.) Analysis of the microstructure indicated small amounts of Si, consistent with chemical analysis and measured lattice constants. Clean $CrSi_2$ surfaces suitable for photoemission studies were prepared by cleaving posts of dimension $\sim4\times4\times10$ mm^3 *in situ* immediately before measurements were undertaken.

The Si-Cr interfaces were also prepared *in situ* by Cr deposition on atomically clean Si(111) surfaces. Si wafers were cleaned for this purpose by standard heat treatments[13] and mild sputtering. Interfaces were prepared with identical results on both Si(111)7×7 and Si(111)1×1 surfaces as distinguished through photoemission.[14] The interface behavior at room temperature was the same as reported previously for interfaces on UHV-cleaved Si single crystals in the metal-coverage range explored here ($\Theta>1$–2 monolayers).[11,12] Total pressure during Cr sublimation from a Ta boat was always better than 2×10^{-10}

 ©1983 The American Physical Society

TABLE I. List of structural parameter for Cr silicides.

	Cr_2Si	CrSi	$CrSi_2$
Crystal structure	cubic *A* 15	cubic *B* 20	hexagonal *C* 40
Space group	*Pm* 3*m*	$P2_13$	$P6_222$
Lattice parameters (Å)	$a=4.5578$	$a=4.607$	$a=4.428$; $c=6.363$
Unit-cell volume ($Å^3$)	94.68	97.78	108.05
Number of molecules/unit cell	2	4	3
Number of shells within 7 Å			
Si-Si	3	9	20
Si-Cr	5	21	12
Cr-Cr	9	9	8
First-neighbor distance (Å)			
Si-Si[a]	3.947	2.846	2.476
Si-Cr	2.548	2.314	2.476
Cr-Cr[b]	2.279	2.825	3.066

[a]2.351 Å in Si.
[b]2.494 Å in Cr.

Torr with recovery to the operating pressure of $\sim 3\times 10^{-11}$ Torr within ~ 1 min after deposition. The metal coverage of the Si substrate, Θ, was monitored with a quartz thickness monitor and is given in terms of the Si(111) surface atomic density ($\Theta=1$ monolayer for 7.6×10^{14} atoms/cm^2). Thermal processing of the interface was performed by electron bombardment on the back of the Si wafer. The sample temperature was monitored with an infrared pyrometer. Fixed annealing temperatures were used ($400 < T < 1100\,°C$), and the annealing time was increased in 10-min cycles until the steady state was reached, as seen from the experimental spectra.

Photoemission measurements were performed using synchrotron radiation from the 240-MeV electron storage ring Tantalus at the University of Wisconsin-Madison and a toroidal grating monochromator. Photoelectron energy distribution curves (EDC's) were recorded with a typical overall resolution (electrons plus photons) of 0.4 eV for the valence-band studies. The Si 2*p* and Cr 3*p* cores were studied at $h\nu=120$ eV ($\sim$0.5-eV resolution) and 78 eV ($\sim$1-eV resolution), respectively. Details of the experimental system have been given in Ref. 15.

III. THEORETICAL TECHNIQUES

The energy-band calculations for Cr_3Si, CrSi, and $CrSi_2$ were based on the linear combination of atomic orbitals (LCAO) method in the extended—Hückel-theory approximation.[16] This semiempirical approach greatly simplifies the computation and allows calculations of the electronic energy levels of complex systems such as the bulk silicides of interest here.[17] The same calculational scheme was previously used for the near-noble-metal silicides, yielding results which were in good agreement with experiment.[8,9,18] A detailed description of the method can be found in Ref. 9.

In these calculations, the atomic valence orbitals ϕ_α are expressed as products of the appropriate spherical harmonics times a radial wave function of the form

$$R_\alpha(r)=c_1\chi_\alpha(\xi_1)+c_2\chi_\alpha(\xi_2)\ ,$$

where $\chi_\alpha(\xi)$ are Slater-type orbitals with orbital exponent ξ.[9] The Slater orbital exponents have been adjusted to reproduce the electronic bands of pure Si (Ref. 19) and Cr (Ref. 20). The resulting value of the parameters ξ_1 and ξ_2 are shown in Table II, together with the constants c_1 and c_2.[21]

The Coulomb integrals $\alpha_i \simeq \langle \phi_i \mid H \mid \phi_i \rangle$ are set equal to the negative of the valence-orbital ionization potential I_i for the δ_i orbital,[22] and the resonance integrals $\beta_{ij}=\langle \phi_i \mid H \mid \phi_j \rangle$ are approximated by[9]

$$\beta_{ij}=-k(I_iI_j)^{1/2}S_{ij}\ ,$$

where S_{ij} are overlap integrals and $k=2.5$, as suggested by Breese and Perkins[23] for metallic systems. The I_i can be interpreted as charge-dependent potentials and an iterative procedure can be built up allowing I_i to vary as

$$I_i(q)=C_i+B_iq\ ,$$

where q is the excess charge per atom. This charge was calculated through a Mulliken population analysis,[24] and the iterative procedure was stopped when the charge variation between two successive iterations was less than 0.005 electrons per atom. The numerical values used for the parameter C_i and B_i (Ref. 25) for the valence orbitals ϕ_i are also shown in Table II.

IV. EXPERIMENTAL RESULTS

Photoelectron energy distribution curves (EDC's) for the valence bands of bulk $CrSi_2$ cleaved *in situ* are shown in Fig. 1 for photon energies between 16 and 120 eV. The EDC's have been approximately normalized to the main emission features and are given in arbitrary units. The Si 2*p* and Cr 3*p* levels are shown in the lower part of the figure for photon energies which give comparable surface

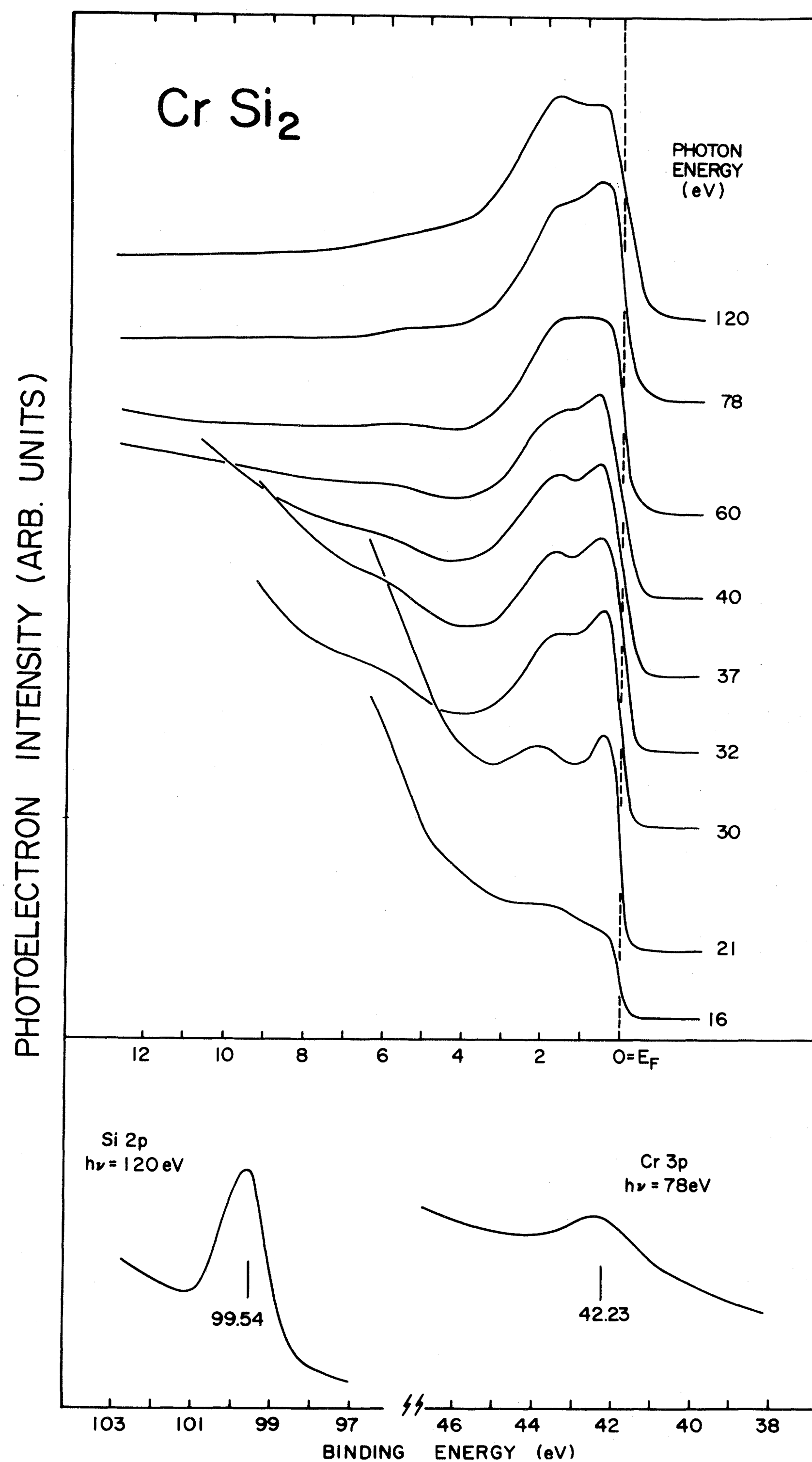

FIG. 1. Valence-band and core-level EDC's for bulk, polycrystal $CrSi_2$ cleaved *in situ*. The measured binding energy of the Si 2*p* (bottom left) and Cr 3*p* (bottom right) cores is indicated in the figure and the corresponding experimental uncertainty is 0.10 and 0.14 eV, respectively.

sensitivities for the Si and Cr core levels (120 and 78 eV). The relative intensity of the two main valence-band spectral features varies with photon energy, particularly at low photon energy where final-state effects are important, but both features show very little dispersion for $h\nu > 25$ eV, and we associate them with structures in the density of states (DOS). The valence-band emission of $CrSi_2$ at $h\nu = 50$ eV, where the metal *d* photoionization cross sec-

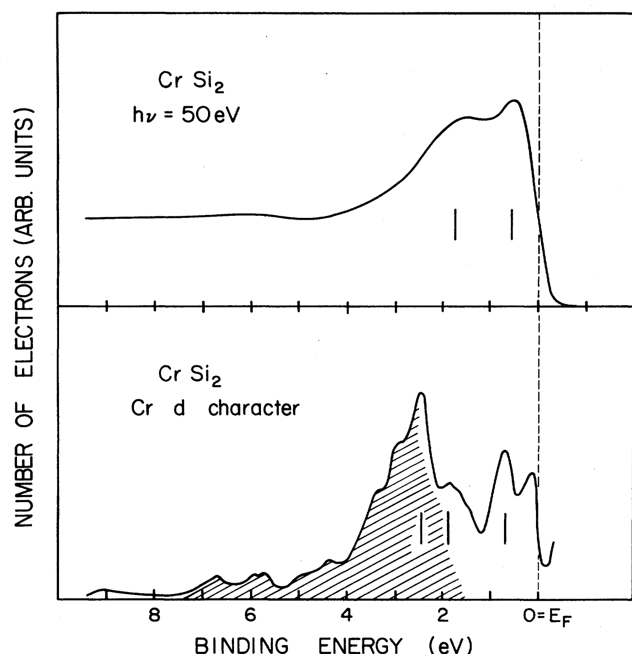

FIG. 2. Comparison of valence-band emission of $CrSi_2$ at $h\nu=50$ eV with the l-projected partial DOS showing the Cr-derived $3d$ character. The shaded area corresponds to the $3d$ states that have hybridized with the Si p states (in bonding combinations). Photoemission emphasizes the nonbonding d features in these $3d$-metal disilicides. The main spectral features 0.6 eV below E_F reflects such states, while important contributions to the broad shoulder centered at 1.7 eV should come from both bonding and nonbonding states.

tion dominates, is compared with the theoretical Cr-derived $3d$ character in Fig. 2. The shaded region corresponds to d states which are hybridized with Si p states. (See the following section.)

The results for the Si(111)-Cr interface are summarized in Figs. 3 and 4. In Fig. 3, the valence band, Si $2p$ and Cr $3p$ core emission from the interface at Cr coverage $\Theta=10$ monolayers is compared with the valence band and core emission of bulk $CrSi_2$. Cr deposition on Si(111)7×7 results in the formation of an extended intermixed Si-Cr phase for $1.5<\Theta<10$ which is identical to what has been discussed for the Si(111)2×1-Cr interface. For $\Theta>10$, a film of unreacted Cr forms over the reacted interface. The effects of annealing 50-Å Cr films evaporated on the Si wafer are shown in Fig. 4. The topmost curve represents the bulk Cr-like emission, and the dotted line superimposed on this spectrum represents bulk $CrSi_2$ from Fig. 1. EDC's displaced downward show the effect of 10-min annealing cycles at successively higher temperature in the range 400—1100 °C. Only at 400 ± 50 °C were two heating cycles needed to reach steady state.

V. THEORETICAL RESULTS

Figure 5 shows the total DOS for Cr_3Si, CrSi, $CrSi_2$ and pure Cr, as calculated with the parameters of Table II. The corresponding DOS projections in Cr-derived d and s-p states are compared with Si-derived s-p states in Fig. 6. These DOS's have been calculated using a mesh of 210 $\vec{k}$ points in the irreducible Brillouin zone for $CrSi_2$ and 84 $\vec{k}$ points for Cr_3Si and CrSi. A broadening of 0.1 eV has

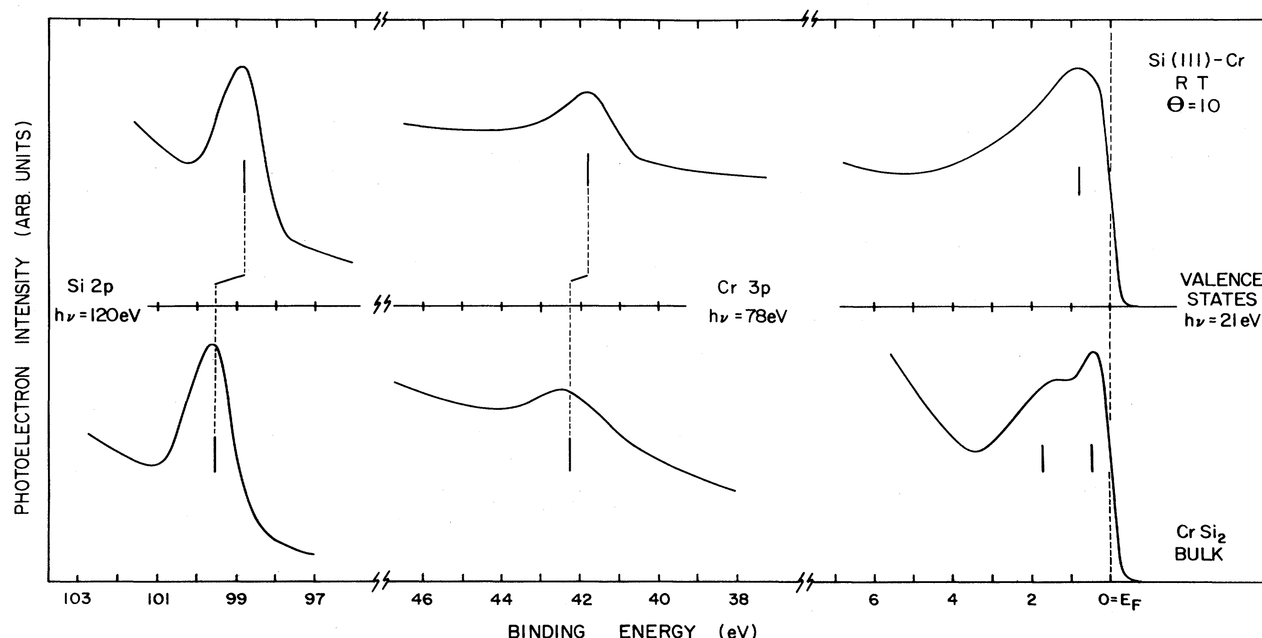

FIG. 3. Comparison of valence band and core emission for $CrSi_2$ to the Si(111)-Cr interface at room temperature and Cr coverage $\Theta=10$ ML. The photon energies have been chosen to obtain similar surface sensitivity for core and valence-band features. The interface reaction products (top) show a clearly different electronic structure with respect to $CrSi_2$, including core-binding energy differences of -0.76 and -0.42 eV, respectively, for the Si $2p$ and Cr $3p$ levels.

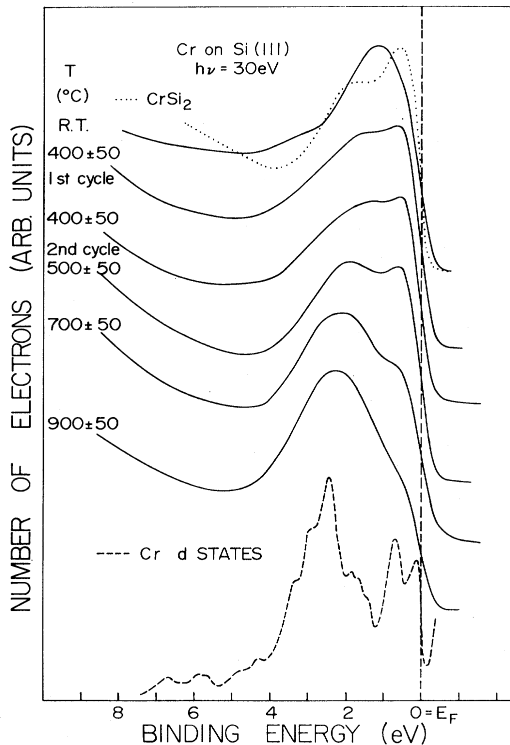

FIG. 4. Valence-band emission at $h\nu=30$ eV of the Si-Cr junction as a function of 10-min annealing cycles at increasing temperature. The topmost solid curve corresponds to a 50-Å Cr film deposited on Si(111) at room temperature. Superimposed on it is an EDC for bulk $CrSi_2$ (dotted line). The bottom-most curve (dashed line) shows for comparison the theoretical Cr-derived $3d$ character. At $\sim$400 °C, a disilicide-like doublet emerges while Cr $3p$ and Si $2p$ core features show binding energies consistent, within experimental uncertainty, with the values observed for bulk $CrSi_2$. Annealing at higher temperatures enhances emission from the Si-metal p-d hybrid states 2–3 eV below E_F (see Fig. 2) and the Si $2p$ and Cr $3p$ core-binding energies remain $CrSi_2$-like. The relative core intensity shows a Si-rich stoichiometry at the surface.

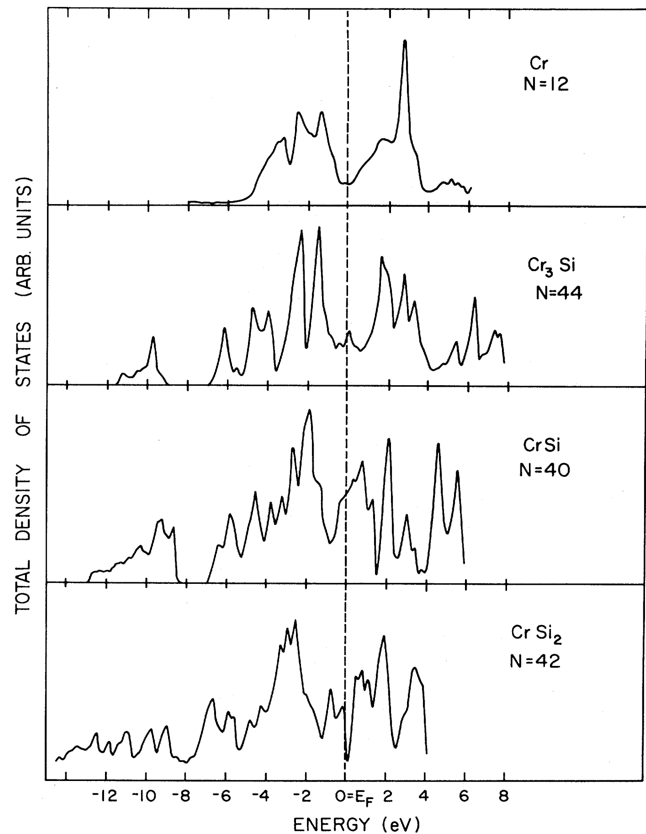

FIG. 5. Total densities of states for Cr and Cr silicides with arbitrary normalization. The corresponding number of states/(eV unit cell) can be obtained through the total number N of valence electrons per unit cell.

been used to obtain the DOS in Figs. 5 and 6. The excess charge per atom,[9] as calculated from the iterative procedure outlined in Sec. III, is the charge transfer per atom due to the Si—Cr chemical bond and is given in Table III.

The total DOS for Cr is very similar to that of Laurent *et al.*[26] Strong $3d$-$3d$ hybridization splits the d bands into two groups of states, with the bonding combination generally below E_F and the antibonding states mostly above E_F. The Fermi level itself falls in a region of low state density.[27] Three main DOS features at about -1.3, -2.5, and -3.5 eV correspond to states of different symmetry[28] and spatial extent.[29] Photoemission clearly emphasizes the structure nearest E_F while the deeper two appear unresolved at $\sim$3 eV.[30]

TABLE II. Input parameters used in the calculations of the electronic structure of Cr silicides. ξ from fitting of the energy bands of elemental Si (Ref. 19) and Cr (Ref. 20), C_1 and C_2 from atomic data tables (Ref. 21), C_i and B_i from Ref. 25.

Valence orbital	Si		Cr		
ϕ_i	$3s$	$3p$	$4s$	$4p$	$3d$
c_1	1.0	1.0	0.4458	1.0	0.4071
ξ_1 (a.u.$^{-1}$)	2.25	1.65	2.70	2.0	4.369
c_2	0	0	0.6433	0	0.7324
ξ_2 (a.u.$^{-1}$)			1.49		1.768
C_i (eV)	14.82	7.75	6.60	3.52	7.18
B_i (eV)	12.39	10.13	7.14	5.90	11.90

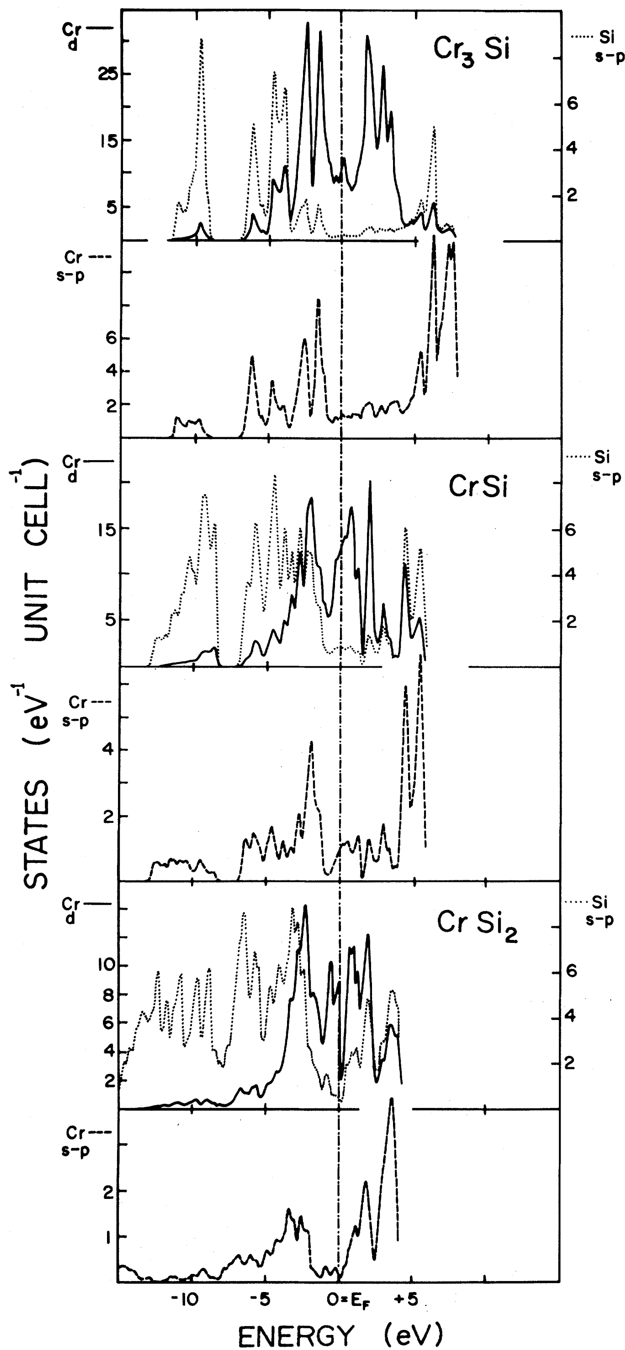

FIG. 6. Partial DOS for Cr silicides showing the *l*-projection of the Cr-derived *d* (solid line) and *s*-*p* (dashed line) character versus the Si-derived *s*-*p* character (dotted line). The chemical bonding depends on the coupling of Cr *d* and Si *p* states. $CrSi_2$ is the only Cr silicide to have dominant nonbonding DOS feature within 1 eV of E_F. The Si *s* states are not directly involved in the bonding and fall more than 8 eV below E_F.

TABLE III. Excess charge Δq for atom as calculated from the iterative procedure outlined in Sec. III. The procedure was stopped when the charge variation between two successive iterations was less than 0.005 electron/atom. The charge transfer is always less than 0.5% of the valence charge/atom for Cr and less than 1% for Si.

Silicide	Δq Cr (electrons/atom)	Δq Si (electrons/atom)
Cr_3Si	-0.013	$+0.038$
CrSi	-0.029	$+0.029$
$CrSi_2$	$+0.015$	-0.007

VI. DISCUSSION

The chemical bond for the Cr and nearly-noble-metal silicides is very similar[8–10,12,31] with coupling of Cr 3*d* and Si *p* states and a reduction of the Si *s*-*p* hybridization. For Cr silicides, many of the occupied 3*d* states bond with Si, and the resulting silicide DOS is determined by two competing trends. First, the Cr-Si hybridization produces bonding features below and antibonding features above E_F, and the 3*d*-band width is broadened. Second, the Cr 3*d*-3*d* interaction is reduced, the electronic configuration becomes more atomic,[8,32] and the 3*d*-band width is reduced. The importance of the first mechanism in determining the valence-band structure is greater than that for the nearly-noble-metal silicides, because there are few occupied *d* states not involved in the bonding with Si (nonbonding *d* states). For the Ni silicides, on the other hand, the narrower nonbonding 3*d* states dominate the EDC's and changes in the Ni-Ni interaction determine most DOS changes in the Ni_2Si-NiSi-$NiSi_2$ series.[8]

Previous DOS calculations for Cr silicides in their real crystal structures exist only for the *A*15 structure Cr_3Si where the total and *l*-projected density of states as obtained by Arbman and Jarlborg[33] are in good agreement with those presented here.[34] In Cr_3Si, the Cr-Cr interaction dominates in determining the electronic structure, and the total DOS in Fig. 5 is reminiscent of the 3*d*-3*d* bonding-antibonding separation in bulk Cr. Indeed, the Cr-derived states between -4 and $+4$ eV do not mix with Si states. The Si—Cr *p*—*d* bonding combinations are evident between -4 and -6.5 eV. The corresponding antibonding states fall more than 4 eV above E_F. As in other metal-rich silicides,[8] the Si sp^3 hybridization is replaced by Si-Cr *p*-*d* coupling and the *s* states form an isolated band around -10 eV.

For CrSi (cubic, *B*20-type structure), the Si-Cr *p*-*d* bonding states appear between -1 and -6 eV, and nonbonding *d* character is present at the Fermi level. The *p*-*d* antibonding states are $\sim$4 eV above E_F, and a gap separates the *s* states from the rest of the DOS, even if the value of the energy separation is decreased with respect to Cr_3Si because of the larger Si-Si interaction. In $CrSi_2$ (hexagonal, *C*40 type) this gap no longer exists, and states more than -7 eV below E_F account for most of the Si-derived *s* character. The *p*-*d* bonding states appear between -1 and -5 eV, and the empty antibonding orbitals now start only $\sim$1 eV above E_F.

The results of Fig. 5 for $CrSi_2$ show that E_F falls in a region of low, but nonzero, state density. Figure 7 shows the DOS near E_F, and the energy bands near E_F are repro-

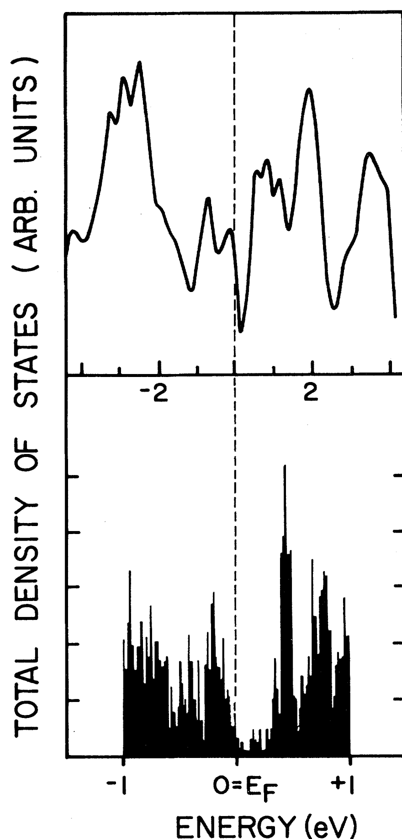

FIG. 7. Detail of the total DOS for $CrSi_2$ near E_F. Top: DOS obtained with a broadening of 0.1 eV. Bottom: High-resolution histogram plot showing the small but finite DOS at E_F.

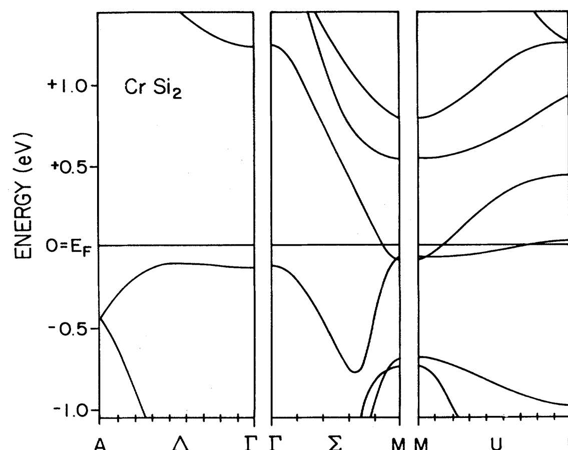

FIG. 8. Energy-band diagram for $CrSi_2$ showing selected energy levels near E_F along high-symmetry lines in the $C40$ structure Brillouin zone. Two bands are shown to cross E_F near the M and L symmetry points. The resulting carrier density is estimated at 8.1×10^{19} carrier/cm^3 and is typical of a semimetal.

duced in Fig. 8. The crossing of the bands near M rules out a forbidden gap and semiconducting behavior for $CrSi_2$. The carrier density in $CrSi_2$ can be estimated by counting the fraction of states involved in the band crossing out of the 2058 $\vec{k}$ points in the Brillouin zone. The resulting estimate of 8.1×10^{19} carrier/cm^3 is typical of a semimetal. (In our investigations, E_F was determined experimentally through measurements of Au and Cr films evaporated *in situ*. The spectra of Fig. 1 are in agreement with the metallic character of $CrSi_2$, showing a low-energy cutoff centered at E_F with a width determined by the experimental resolution.[35] The low calculated carrier density may explain why $CrSi_2$ has been reported to be a metal by some authors and a small-gap semiconductor by others.[36])

Our calculations show little charge transfer for these three silicides, always less than 1% of the valence charge/atom for Cr to Si in Cr_3Si and CrSi and completely negligible in $CrSi_2$ (see Table II). This suggests that ionicity is a minor contributor to the bond. Our calculated charge transfer for Cr_3Si appears in contrast to the large charge transfer from Si to metal suggested by Staudemann[37] and Mattheiss and Hamann.[38] However, as discussed by Pickett *et al.*,[39] numerical values depend on the method used to separate the space around the Si or metal atoms. This problem does not exist for our LCAO decomposition and, furthermore, our calculated charge transfer is consistent in magnitude and sign with the electronegativity difference (Pauling electronegativity is 1.6 for Cr and 1.8 for Si).

Previous calculations for the Cr_3Si, CrSi, and $CrSi_3$ in the Cu_3Au and CuAu structures showed qualitatively the same chemical bonding as the present calculations, i.e., Si-Cr p-d coupling, removal of Si sp^3 hybridization, and small charge transfer.[12] The present results show a general lowering of the $3d$-derived occupied DOS for CrSi and $CrSi_3$. We suggest that such differences arise from the use of the real silicide geometry in the present calculations.

The disilicide of Cr is of special interest since it is the only Cr silicide known to grow on Si upon reaction[2] at 450°C. In previous work, however, we demonstrated[8] that room-temperature deposition of Cr onto cleaved Si resulted in intermixing for Cr coverages up to 10 monolayers (ML). This reacted layer constitutes the "real" interface between Si and Cr and is gradually covered with unreacted metal upon further Cr deposition. The implication is, of course, that this reacted layer determines the junction profile and transport properties of any macroscopic Si-Cr junction. Therefore, after examining in Fig. 2 the electronic structure of $CrSi_2$ on the basis of our theoretical calculations, we compare in Fig. 3 the properties of $CrSi_2$ with those of the interface reaction product for $\Theta=10$ ML. The valence states of $CrSi_2$ show a main peak at 0.6 eV and a broad shoulder at about 1.7 eV (extending between 1.3 and 3 eV). Our calculations predict a main nonbonding $3d$ feature 0.65 eV below E_F, while important contributions to the broad shoulder extending between 1.3 and 3 eV come from the $3d$ bonding states at 2.4 eV in the calculations and from the nonbonding $3d$ states around 1.8 eV. The identification is in agreement with the sys-

tematic trend in the DOS of the $3d$ metal disilicides (Ref. 40) and confirms that ultraviolet photoemission emphasizes the nonbonding $3d$ features with respect to the d states directly involved in the bond with Si.

For Cr deposition onto Si(111) (Fig. 3), the Cr-derived $3d$ states quickly dominate the valence-band emission and give rise to a broad maximum that shifts with coverage toward E_F until the fully reacted layer is formed ($\Theta = 10$ ML). Comparison of the valence bands of the interface reaction products and bulk $CrSi_2$ shows that the double $3d$ structure (0.6 and 1.7 eV) characteristic of the disilicide is not present for the interface and only a broad $3d$ peak appears at 0.75 eV in the interface spectrum (full width at half maximum of 2.6 eV compared to 2.1 eV for $CrSi_2$).

The binding energies of the Si $2p$ and Cr $3p$ cores are important in gauging interface reaction. The Cr $3p$ and Si $2p$ cores both shift toward lower-binding energy for coverages $1 < \Theta < 10$ and for $\Theta \geq 10$ stabilize at 41.8 ± 0.1 and 98.80 ± 0.1 eV below E_F.[41] Analogous results for $CrSi_2$ show a binding energy of 99.54 ± 0.1 eV for the Si $2p$ and 42.23 ± 0.14 eV for the Cr $3p$, identical within experimental uncertainty to the $3p$ core binding energy in bulk Cr.[42] Therefore, the interface-reaction product exhibits Si $2p$ and Cr $3p$ core shifts of 0.74 and 0.42 eV to lower binding energy relative to $CrSi_2$, indicating that the electronic configuration differs substantially from $CrSi_2$.

Examination of the theoretical Cr-Si results of Fig. 7 shows that only $CrSi_2$ exhibits dominant $3d$ nonbonding DOS features within 1 eV of E_F. Since the photoemission results for all $3d$ metal silicides[40] are in good agreement with $3d$-projected densities of states where the nonbonding d character is emphasized, we conclude that *none* of the bulk Cr silicides examined theoretically exhibits electronic structure sufficiently close to the interface-reaction product to allow unambiguous identification. Clearly, what is needed is direct insight into the structural character of the interface so that theoretical modeling can be more specific.

To examine whether the interface layer would evolve to $CrSi_2$ upon thermal treatment, we annealed 50-Å Cr films on Si(111) and monitored the valence-band and core-level features. In particular, annealing temperatures in the 400—1100 °C range were emphasized because Rutherford backscattering and x-ray-diffraction investigations[2,43] have shown $CrSi_2$ to be the only growth phase to form at the interface. The topmost curve of Fig. 4 represents a thick Cr film on Si(111). Annealing at 400 ± 50 °C gives strong Si $2p$ emission 99.45 ± 0.14 eV below E_F and shifts the Cr $3p$ cores from the Cr metal position of 42.22 eV to 42.14 ± 14 eV, converging on the values of 99.54 ± 0.10 and 42.23 ± 0.14 eV observed for bulk $CrSi_2$. Correspondingly, the valence-band emission becomes $CrSi_2$-like, though the spectral features are broader. Annealing above 500 °C results in the emergence of enhanced emission 2—3 eV below E_F. Above ~ 700 °C, this new feature dominates, and the $3d$ nonbonding structure near E_F is only a weak shoulder.

These modifications of the valence states result from the formation of a Si-rich silicide at the surface. Enhanced emission 2—3 eV below E_F reveals an increased number of Si-Cr p-d hybrid orbitals relative to the nonbonding d states. Further, the ratio of the integrated emission from Si $2p$ and Cr $3p$ cores is 1.8 times higher for the 600 ± 50 °C annealed interface silicide than for cleaved $CrSi_2$, indicating a marked enrichment in the Si concentration. Finally, throughout the high-temperature annealing cycles, during which the valence states are modified, the Si $2p$ and Cr $3p$ cores maintain the bulk $CrSi_2$ binding energy (experimental scatter of ~ 0.1 eV). Low-energy electron diffractive and Auger studies of $CrSi_2$ nucleation on Si(111) by Oura *et al.* suggested that annealing above 600°C—900°C produces several atomic layers of silicon over a crystalline silicide layer. Our results confirm the increase in the Si surface concentration but show that the Si-Cr bonding remains fundamentally $CrSi_2$-like, with no evidence of formation of several layers of *elemental* silicon at the surface. This is also consistent with analogous studies of Pd_2Si.[44]

The results of Fig. 6 are important in discussions of room temperature Si-Cr interface reaction. We have shown that a $CrSi_2$-like phase nucleates at relatively low temperature (400 ± 50 °C) and that this phase, while lacking long-range order,[45] exhibits characteristic $CrSi_2$-like valence and core features. Therefore, both experimental and theoretical results indicate that the room-temperature interface-reaction product is not simply a disordered $CrSi_2$ phase.

Finally, we observe that the Si-rich $CrSi_2$ phase shows characteristic enhancement of the valence-band emission 2—3 eV below E_F while exhibiting a bulk $CrSi_2$-like binding energy for the Si $2p$ and Cr $3p$ cores. Therefore, unlike the case of the Si(111)-Pd interface where room-temperature reactions seem to yield a locally Si-rich Pd_2Si phase, we find evidence that room-temperature Si(111)-Cr interface reaction does not yield a nonstoichiometric version of $CrSi_2$, the first silicide-nucleation phase.

The understanding of Si-metal interface reaction requires the characterization of the interface-reaction products as a function of the various reaction parameters, including temperature and metal coverage. We have sought to show how a systematic experimental and theoretical investigation of the electronic properties of interface and bulk Si-metal compounds can increase our understanding of both interface morphology and of the parameters, such as long-range order and stoichiometry variation, that affect the silicide-electronic structure.

ACKNOWLEDGMENTS

This work was supported by the U. S. Army Research Office under Contract No. DAAG29-83-K-0061. The Synchrotron Radiation Center, University of Wisconsin is supported by the National Science Foundation under Grant No. DMR-80-20164, and we acknowledge the warm hospitality and cheerful support of that laboratory. We gratefully acknowledge the expert sample preparation and characterization work by O. D. McMasters of Ames Laboratory. The work at the University of Modena was supported by the Centro di Calcopo Universitá di Modena. One of us (F.A.S.) acknowledges support of the U.S. Department of Energy Contract No. W-7405-ENG-82.

[1]S. P. Muraka, J. Vac. Sci. Technol. 17, 775 (1980); G. Ottaviani, *ibid*. 18, 924 (1981).

[2]K. N. Tu, in *Thin Film Interdiffusion and Reactions*, edited by J. M. Poate, K. N. Tu, and J. W. Mayer (Wiley, Chichester, England, 1978).

[3]K. N. Tu, Appl. Phys. Lett. 23, 493 (1973).

[4]J. E. Rowe, S. B. Christman, and G. Margaritondo, Phys. Rev. Lett. 35, 1471 (1975); G. Margaritondo, J. E. Rowe, and S. B. Christman, Phys. Rev. B 14, 5396 (1976).

[5]L. Braicovich, I. Abbati, J. N. Miller, I. Lindau, S. Schwarz, P. R. Skeath, C. Y. Su, and W. E. Spicer, J. Vac. Sci. Technol. 17, 1005 (1980); I. Abbati, L. Braicovich, and B. De Michelis, Solid State Commun. 36, 145 (1980).

[6]J. L. Freeouf, G. W. Rubloff, P. S. Ho, and T. S. Kuan, Phys. Rev. Lett. 43, 1836 (1979); P. S. Ho, P. E. Schmid, and H. Foll, *ibid*. 46, 782 (1981).

[7]P. J. Grunthaner, F. J. Grunthaner, A. Madhukar, and J. W. Mayer, J. Vac. Sci. Technol. 19, 649 (1981); N. W. Cheung, P. J. Grunthaner, F. J. Grunthaner, J. W. Mayer, and B. M. Ullrich, *ibid*. 18, 917 (1981).

[8]J. H. Weaver, V. L. Moruzzi, and F. A. Schmidt, Phys. Rev. B 23, 2916 (1981); A. Franciosi, J. H. Weaver, and F. A. Schmidt, *ibid*. 26, 546 (1982).

[9]O. Bisi and C. Calandra, J. Phys. C 14, 5479 (1981); O. Bisi and L. W. Chiao, Phys. Rev. B 25, 4943 (1982).

[10]Y. Chabal, J. E. Rowe, J. M. Poate, A. Franciosi, and J. H. Weaver, Phys. Rev. B. 26, 2748 (1982); A. Franciosi, J. H. Weaver, Y. Chabal, J. E. Rowe, and J. M. Poate, J. Vac. Sci. Technol. 21, 624 (1982).

[11]A. Franciosi, D. J. Peterman, and J. H. Weaver, J. Vac. Sci. Technol. 19, 657 (1981).

[12]A. Franciosi, D. J. Peterman, J. H. Weaver, and V. L. Moruzzi, Phys. Rev. B 25, 4981 (1982).

[13]See, for example, D. E. Eastman, J. Vac. Sci. Technol. 17, 492 (1980), and references therein.

[14]D. E. Eastman, F. J. Himpsel, and J. F. van der Veen, Solid State Commun. 35, 345 (1980).

[15]G. Margaritondo, J. H. Weaver, and N. G. Stoffel, J. Phys. E 12, 662 (1979).

[16]R. Hoffman, J. Chem. Phys. 39, 1397 (1963).

[17]A summary of the structural properties of $CrSi_2$, CrSi, and Cr_3Si is given in Table I. As for many other silicides, the large number of atoms per unit cell and the complex crystal structure make first-principles calculations difficult and fairly expensive. Semiempirical approaches or calculations based on simplified lattice structures are often used to gain insight into the character of the metal—silicon bond.

[18]P. S. Ho, G. W. Rubloff, J. E. Lewis, V. L. Moruzzi, and A. R. Williams, Phys. Rev. B 22, 4784 (1980).

[19]J. R. Chelikowski and M. L. Coehn, Phys. Rev. B 14, 556 (1976).

[20]R. P. Gupta and S. K. Sinha, Phys. Rev. B 3, 2401 (1971).

[21]Values taken from tables of atomic wave functions: E. Clementi and C. Roetti, At. Data Nucl. Data Tables 14, 177 (1974).

[22]H. Basch, A. Viste, and H. B. Gray, J. Chem. Phys. 44, 10 (1966).

[23]A. Breeze and P. G. Perkins, J. Phys. F 5, 255 (1975).

[24]R. S. Mulliken, J. Chem. Phys. 23, 1833 (1955).

[25]The parameters were taken from atomic spectra data of H. Basch, A. Viste, and H. B. Gray, J. Chem. Phys. 44, 10 (1966); R. C. Baetzold, *ibid*. 55, 4355 (1971).

[26]D. Y. Laurent, J. Callaway, J. L. Fry, and N. E. Breuer, Phys. Rev. B 23, 4977 (1981).

[27]The bonding-antibonding splitting differs from the crystal-field splitting that removes the degeneracy of states with t_{2g} (xy,yz,xz) and e_g $(x^2-y^2,3z^2-r^2)$ symmetry in a cubic environment. In fact, the average contribution to the 3*d* DOS below E_F is of the same order of magnitude for t_{2g} (22.6%) and e_g (16%) states.

[28]The LCAO analysis shows that the structure at -1.3 eV is approximately 82% t_{2g} character while those at -2.5 and -3.5 eV have approximately 60% t_{2g} and 40% e_g character.

[29]The states that lie deeper in energy exhibit larger radial extension. See K. M. Ho, B. N. Harmon, S. H. Liu, and S. K. Sinha, Phys. Rev. B 14, 1283 (1976).

[30]Results for Cr films evaporated on inert substrates are in good agreement with data for bulk Cr samples. See. J. Barth, F. Gerken, K. L. I. Kobayashi, J. H. Weaver, and B. Sonntag, J. Phys. C 13, 1369 (1980).

[31]P. S. Ho, G. W. Rubloff, J. E. Lewis, V. L. Moruzzi, and A. R. Williams, Phys. Rev. B 22, 4784 (1980).

[32]A. R. Williams and N. D. Lang, Phys. Rev. Lett. 40, 954 (1978).

[33]G. Arbman and T. Jarlborg, Solid State Commun. 26, 857 (1978); T. Jarlborg, J. Phys. F 9, 283 (1979).

[34]Some differences do exist with respect to Ref. 33 for the 3*d*-derived DOS *above* E_F. This is not surprising since our LCAO calculations are better suited to reproduce the ground state of the system.

[35]Valence-band photoemission, however, may not discriminate between a metal and a semiconductor with band bending in the near-surface region.

[36]J. P. Suchet, *Crystal Chemistry and Semiconduction in Transition Metal Binary Compounds* (Academic, New York, 1971), p. 101.

[37]J. L. Staudenmann, Solid State Commun. 23, 121 (1977).

[38]L. Mattheiss and D. Hamann, Solid State Commun. 38, 689 (1981).

[39]W. E. Pickett, K. M. Ho, and J. L. Cohen, Phys. Rev. B 19, 1734 (1979); 19, 1751 (1979).

[40]J. H. Weaver, A. Franciosi, and V. L. Moruzzi (unpublished) discuss bonding for the silicides of Ca through Cu. A brief preliminary report appeared as A. Franciosi and J. H. Weaver, Physica 117&118B, 846 (1983).

[41]We did not attempt a deconvolution of the spin-orbit components of the Si 2*p* and Cr 3*p* doublets. The quoted binding energies correspond to the peak intensities with respect to a linearly extrapolated secondary background.

[42]For a ~300-Å-thick Cr film evaporated on oxidized Ta substrate we obtained E_B $(3p)=42.22\pm0.10$ eV, in good agreement with the most recent x-ray photoelectron spectroscopy results of 42.3 eV from A. Lebugle, W. Axelsson, R. Nyholm, and N. Mårtensson (unpublished).

[43]R. W. Bower and J. W. Mayer, Appl. Phys. Lett. 20, 359 (1972); J. W. Mayer and K. N. Tu, J. Vac. Sci. Technol. 11, 86 (1974).

[44]See A. Franciosi and J. H. Weaver, Phys. Rev. B 27, 3554 (1983), and detailed references therein.

[45]K. Oura, S. Okada, and T. Hanawa, in Proceedings of the 8th International Vacuum Congress, Cannes (France), 1980, edited by F. Abeles and M. Croset [Suppl. à la Revue Le Vide, Les Couches Minces 201, 181 (1981)].